Mixing Phosphors to Improve the Temperature Measuring Quality

Paulina Bolek[1,*], Justyna Zeler[1,2], Luís D. Carlos[1,2,*], and Eugeniusz Zych[1,2]

[1] University of Wroclaw, Faculty of Chemistry, 14. F. Joliot-Curie Street, 50-383 Wroclaw, Poland

[2] Phantom-g, CICECO-Aveiro Institute of Materials, Physics Department, University of Aveiro

3810-193 Aveiro, Portugal

keywords: luminescence thermometry, mixed phosphors, dual-mode thermometer, bandgap engineering, YAG, Pr^{3+}

Abstract

Using luminescent materials for temperature measuring is considered the perspective remote technique nowadays. Designing new materials which combine a wide operating range with satisfying relative thermal sensitivity (S_r) and temperature uncertainty values is still a challenge. In this paper, we study the luminescence properties and thermometric performance of a mixture of two phosphors. These are Ga-modified garnets - $Y_3(Al_3Ga_2)O_{12}$:0.1%Pr and $Y_3(Al_1Ga_4)O_{12}$:0.1%Pr - already reported as dual-mode luminescent thermometers. We show a new concept to improve important thermometric parameters of luminescence thermometers. We prove that such a mixture offers a significantly flatter course of the relative thermal sensitivity vs. temperature with S_r around 1%K^{-1} over a broad temperature interval. Independently of which of the thermometric parameter (Δ_1-Δ_3) is used, temperature measurement may be easily executed in the broad range of temperatures, 15-675 K. At the core of our concept is the use of two phosphors of the same crystal structure. This allows for the equally effective excitation of the two components of the mixture, while both use the same activator.

Introduction

The research of luminescence thermometry continuous its impressive development. New materials showing attractive, sometimes spectacular performance in this remote temperature measuring technique are reported

once in a while [1–5]. The anticipated uses are diverse and aim into applications in biology, medicine, micro- and nano-electronics, aviation, and space research, among others [6–8]. Luminescence thermometry is an attractive technique of temperature sensing because the measurements are not perturbed by external electric or magnetic fields or stray light. Furthermore, the availability of highly sensitive detectors of photons allows to detect of even low-intensity luminescence. A more thorough discussion of those topics one may find in recently published books and reviews [2,5,8–10]. It is obvious that specific applications will require dedicated luminescence thermometers. Some uses - aviation, space research, nuclear power plants – will require good performance in a broad range of temperatures. Yet, it is a challenge to fulfill such requirements maintaining good sensitivity and resolution (accuracy) of measurements.

Significant progress in measuring range, thermal sensitivity, and resolution was simultaneously attained when the intra-configurational 5d→4f UV luminescence of Pr^{3+} ion was exploited together with its 4f→4f emissions in bluish-green (due to the luminescence from the $^3P_0$ level) and red (from $^1D_2$) [11,12]. Moreover, the excitation employing the allowed 4f→5d absorption transition of Pr^{3+} permitted for efficient luminescence with a high signal-to-noise ratio. Such excitation allows using cheap standard excitation light sources without sacrificing the quality of measured spectra which transfers directly to low inaccuracies of temperature sensing. Using this approach, such luminescence thermometers as $Y_3(Al,Ga)_5O_{12}$:Pr [11], $CaSc_2O_4$:Pr [12], Sr_2GeO_4:Pr [13] and $Lu_2(Ge,Si)O_5$:Pr [14], were found to offer both high relative sensitivity (S_r) and high resolution of temperature measurement.

Due to the unavoidable thermal quenching of the 5d→4f luminescence, the operating range using the 5d→4f/4f→4f luminescence intensity ratio (LIR) method [2,4] appeared limited to about 400 degree; occasionally up to 600 degree range but at the expense of lower accuracy. Using solely the temperature-dependence of the 5d→4f luminescence decay time, the 300-400 degree range could be covered. Furthermore, the high relative sensitivity is often offered only within a quite narrow range of temperature while within other fractions of the operating range it is moderate at most. Getting a flatter course of S_r over

the whole operating range, even a few hundred degrees would be very much beneficial. It was challenging to look for a method to overcome this limitation and this paper presents such a possibility employing garnets as an illustrative example.

It was shown that the operating range of such luminescence thermometers as $Y_3(Al,Ga)_5O_{12}$:Pr, $Lu_2(Si,Ge)O_5$:Pr and $Sr(Si,Ge)O_4$:Pr [11,14,15] could be tailored utilizing the band-gap engineering approach, hence, changing the Al:Ga or Si:Ge ratio. This methodology significantly broadened the potentiality of designing better luminescence thermometers and allowed shaping their properties by means of fine-control of the temperature-dependent luminescence processes. Nevertheless, the above-mentioned weaknesses of such thermometers have not been annulled. We believe that this work shows how to undermine this problem – designing a luminescence thermometer whose sensing spans a broad range of temperatures while offering still sufficient relative sensitivity over its whole operating range.

Comparison of the relative sensitivity of $Y_3(Al,Ga)_5O_{12}$:Pr [11] garnets with different Al:Ga ratio (see **Figure 1**) led us to an intriguing conclusion. We noted that a mixture of two deliberately selected phosphors from the family might allow getting a new and promising luminescence thermometer. Its performance could be then controlled by exploiting the 5d→4f/4f→4f and, possibly, 4f→4f/4f→4f LIR over a broader range of temperatures than in the case of the individual phosphors and, equally importantly, with more balanced performance.

One may find in literature scarce examples of similar approaches [16–19]. However, in the previous cases, the mixed phosphors utilized different emitting ions and, in most instances, also the hosts were completely different materials, both in terms of their chemical compositions and crystallographic structures. This approach, thus, has obvious limitations such as, for example, to find an optimal excitation wavelength (energy) for the two different emitting centers or the restricted number of possible pairs of luminescent ions/phosphors that can be used.

In the present research, we thus followed a different strategy. Having chemically very similar phosphors from the $Y_3(Al,Ga)_5O_{12}$:Pr garnet family (differing in the Al:Ga ratio only) and utilizing the same activator, Pr^{3+} ion, we could be sure that any phosphor of the family would be equally effectively excited with the same radiation wavelength. Furthermore, the excitation through the allowed 4f→5d transition assures efficient luminescence, which, in turn, attests a high resolution (low uncertainty) of temperature measurement [11]. Since already the single phosphors from the $Y_3(Al,Ga)_5O_{12}$:Pr family showed interesting performance as thermometers [11], our approach was especially justified.

To demonstrate the plausibility of our approach, two phosphors from the family of garnets were chosen to formulate the mixture: $Y_3(Al_3Ga_2)O_{12}$:0.1%Pr and $Y_3(Al_1Ga_4)O_{12}$:0.1%Pr (hereafter termed YAGG-mix). The reasoning behind our approach is clear from **Figure 1**. The $Y_3(Al_3Ga_2)O_{12}$:0.1%Pr was supposed to assure significant relative sensitivity at cryogenic temperatures, while the $Y_3(Al_1Ga_4)O_{12}$:0.1%Pr was chosen to secure good relative sensitivity above 300 K. It could be expected that utilizing the 5d→4f/4f→4f LIR, a mixture of the two carefully selected phosphors should offer an even broader operating range than single phosphors using the same 5d→4f/4f→4f LIR. Obviously, this could happen only at the expense of the maximum value of the relative sensitivity (S_m).

Experimental section

Materials preparation: The powders of $Y_3(Al_3Ga_2)O_{12}$:0.1mol%Pr and $Y_3(Al_1Ga_4)O_{12}$:0.1mol%Pr were prepared using flux-aided synthesis, as presented in [11]. The YAGG-mix was obtained by thoroughly mixing the two phosphors in the 2:1 weight ratio in an agate mortar. The weight ratio was chosen to analyze the temperature dependence of photoluminescence and thermometric performance of the individual garnets. Namely, the double weight of $Y_3(Al_3Ga_2)O_{12}$:0.1mol%Pr was used due to its lower sensitivity compared to the $Y_3(Al_1Ga_4)O_{12}$:0.1mol%Pr garnet.

Photoluminescence: Photoluminescence excitation and photoluminescence spectra, as well as decay kinetics curves, were measured with an FLS 1000 Spectrometer from Edinburgh Instruments Inc. equipped

with a 450 W Xenon arc lamp for continuous excitation. The equipment was combined with a closed-cycle helium cryostat with a Cu holder for a sample mounting. The spectra were recorded in the 15–675 K temperature range with the 25 K step using a PMT-900 photomultiplier thermoelectrically cooled to -20 °C with a Peltier module and operating in the range 185–900 nm. The double-grating 2x 325 mm Czerny-Tuners excitation and emission monochromators were utilized in the excitation and emission channels. The slits were 0.25 nm and the step was 0.15 nm. Photoluminescence excitation spectra were corrected for the incident light intensity and photoluminescence spectra for the wavelength dependence of the spectral response of the recording channel. The time-resolved emission spectra (TRES) were taken upon the 60 W Xe pulse lamp excitation. The EPLED-280 (280 nm) pulse laser was used to excite the phosphors to measure the decay kinetics curves of the 5d→4f luminescence of Pr^{3+}. The emitted light was then recorded using a TCSPC technique and a high-speed low-noise F-G05 detector featuring a Hamamatsu H5773-04 photomultiplier and covering the 230-870 nm spectral range.

Thermometric Analysis: Detailed description of the thermometric analysis may be found in the previously published paper [11]. Here, we present the most important aspects of the procedure. All photoluminescence spectra were converted from the photon flux per constant wavelength interval function (as measured) into the photon flux per energy interval according to the Jacobian transformation [5,20–22]. The thermometric parameter, Δ, was defined as a ratio of integrated intensities of two specified luminescence bands (I_i and I_j, see **Eq. (1)**) as a function of temperature:

$$\Delta = \frac{I_i}{I_j}. \qquad \textbf{(1)}$$

The relative uncertainty in Δ was determined using **Eq. (2)** [2]:

$$\frac{\delta\Delta}{\Delta} = \sqrt{\left(\frac{\delta I_1}{I_1}\right)^2 + \left(\frac{\delta I_2}{I_2}\right)^2}, \qquad \textbf{(2)}$$

where $\delta I/I$ represents the relative uncertainty in the integrated area that is estimated using the signal-to-noise ratio of the emission spectra. Finally, empirical 2nd-degree polynomial functions were fitted to the experimental data to get the $\delta I/I$ temperature dependence.

The main thermometric parameters defining the thermometer performance, the relative thermal sensitivity (S_r), and the temperature uncertainty (δT), were calculated according to the Eqs. **(3) and (4)**, respectively [2,23,24]

$$S_r = \frac{1}{\Delta}\left|\frac{\partial \Delta}{\partial T}\right|, \quad \text{for intensity ratio} \qquad S_r = \frac{1}{\tau}\left|\frac{\partial \tau}{\partial T}\right|, \quad \text{for lifetime} \qquad \textbf{(3)}$$

$$\delta T = \frac{1}{S_r}\frac{\delta \Delta}{\Delta}, \quad \text{for intensity ratio} \qquad \delta T = \frac{1}{S_r}\frac{\delta \tau}{\tau}, \quad \text{for lifetime} \qquad \textbf{(4)}$$

where τ is the decay time of the 5d→4f luminescence and $\delta\tau/\tau$ its relative uncertainty. The thermometers are out of the operating range when the difference between consecutive Δ or τ measurements in the acquisition of the respective calibration curve does not surpass their corresponding uncertainties $\delta\Delta$ or $\delta\tau$ [8]. To calculate $\delta\tau/\tau$ we fitted the experimental $\delta\tau/\tau_{max}$ values using polynomial functions (τ_{max} is the maximum value of the lifetime of the YGG-mix).

Results and discussion

Temperature dependence of photoluminescence of the YAGG-mix

The excitation spectra of the 606.3 nm luminescence ($^1D_2 \rightarrow {}^3H_4$) (**Figure 2a**) taken at various temperatures consist of a broad band in the ultraviolet range of spectrum peaking at 278 nm - a result of the Pr^{3+} $4f^2 \rightarrow 5d^1f^1$ transition - and narrow lines of lower intensities at about 450-500 nm, which are connected with the $^3H_4 \rightarrow {}^3P_J$ transition of the activator. Around 580-600 nm, low-intensity lines resulting from the $^3H_4 \rightarrow {}^1D_2$ excitation are also seen. Under 280 nm excitation, the YAGG-mix exhibits the strong broad-band 5d→4f luminescence in the UV and narrow emission features in the visible part of the spectra (**Figure 2b,** note the

normalization at 486.0 nm). The latter are related to the $^3P_J \rightarrow {}^3H_4$ radiative transitions (480-550 nm and above ~610 nm) and the $^1D_2 \rightarrow {}^3H_{4,5}$ (580-700 nm). The relative intensities of the luminescence bands change as the temperature increases from 15 to 675 K.

While in the bluish-green range the emission comes exclusively from the $^3P_J \rightarrow {}^3H_4$ transition of Pr^{3+}, in the red (600-640 nm) the luminescence is a superposition of two emissions: from $^3P_0$ and $^1D_2$ levels of Pr^{3+}. Parity-forbidden, but spin-allowed luminescence from the $^3P_0$ level decays much faster than the spin- and parity-forbidden emission from the $^1D_2$ level. **Figure 2c** presents a set of the spectra resulting from the TRES experiment. Clearly, the slower-decaying $^1D_2 \rightarrow {}^3H_{4,5}$ luminescence is located in the 604-612 nm range of wavelengths mainly. This finding appears very useful in the thermometric analysis as presented and discussed in the previous papers [11,15].

Compared to the spectra of the single compositions analyzed previously [11], the striking difference is that the YAGG-mix presents the 5d→4f luminescence throughout the whole range of accessible temperatures, from 15 to 675 K. Furthermore, the relative intensity of the inter- and intra-configurational transitions change continuously spanning the whole investigated range (**Figure 2c**). The most intense 5d→4f luminescence is observed at 15 K, and with increasing temperature, its relative intensity decreases gradually. Bluish-green and red emissions from the $^3P_0$ and $^1D_2$ levels, respectively gain some intensities with temperature as will be seen and discussed later. Note that with increasing temperature especially the red luminescence from the $^1D_2$ is getting relatively stronger, particularly above ~550 K, see **Figure 2b**. Clearly, both the bluish-green and the red emission could be registered at much higher temperatures yet – beyond the limit of our setup. These observations open the door for temperature reading even above 700 K.

Replacing Al with Ga in $Y_3(Al,Ga)_5O_{12}$:0.1%Pr garnets significantly impacts not only the host band-gap but also energies of the host lattice vibrations as discussed in detail previously [11]. This affects the efficiency of the non-radiative relaxation processes, which are directly responsible for intensities of the

various transitions under interest. With increasing Ga-content the available phonons become less energetic [11] hindering the non-radiative multiphonon relaxation, among others between the $^3P_0$ and $^1D_2$ luminescent levels of the Pr^{3+} ion, and this affects their intensities.

In the YAGG-mix, the band-gap engineering appears beneficial from the point of view of luminescence thermometry. Its 5d→4f luminescence is observed up to 675 K. In the cryo-range from both components and at higher temperatures basically from the $Y_3(Al_3Ga_2)O_{12}$:0.1%Pr phosphor. In the latter case, the $Y_3(Al_1Ga_4)O_{12}$:0.1%Pr assures significant intensity of the 4f→4f emissions. These properties directly impact the capability of sensing temperature which will be seen in the thermometric analysis presented later.

Figure 3a shows the temperature dependence of decay curves of the 5d→4f luminescence. In **Figure 3b** decay times derived from these data are presented. Experimental decay traces were fitted using **Eq. (5).**

$$I(t) = A_0 + \sum_{i=1}^{N} A_i \times \exp\left(-\frac{t}{\tau_i}\right), \qquad \textbf{(5)}$$

where *I(t)* represents intensity after time *t*, A_i is a fitting parameter (accounts for the weight of the i-th component in the fit), τ_i is the decay time of the i-th component, and A_0 is a background intensity. While, in general, two components (*N=2*) were needed to get good fits, the deviation from the single-exponential decay was only small at all temperatures. The divergence from the single-exponential kinetics cannot surprise, as the two phosphors forming the YAGG-mix under investigation show individually obviously different dependence on their luminescence decay kinetics on temperature [11].

At 15 K the decay time of the 5d→4f luminescence of the YAGG-mix is 19±0.04 ns and up to about 250 K it shortens only slightly to 18±0.07 ns. This is too little change to be useful for thermometry in this range of temperatures using the decay time as the thermometric parameter. The quenching temperature, $T_{50\%}$, the temperature at which the decay time drops to half of its low-temperature value, is 540 K. As expected, the

quenching extends over a broader range of temperatures than in the case of the individual garnet phosphors: $Y_3(Al_3Ga_2)O_{12}$:0.1%Pr and $Y_3(Al_1Ga_4)O_{12}$:0.1%Pr. This is exactly what we wanted to attain as discussed in the Introduction [11].

Thermometric performance of the YAGG-mix garnet

The YAGG-mix presents strong photoluminescence with significant temperature-dependence of the spectra and decay times of the 5d→4f luminescence as discussed above. Consequently, both LIR and variation of the decay time of the 5d→4f emission with temperature will be evaluated as thermometric parameters of the YAGG-mix.

Figure 4a presents the luminescence spectrum registered at 300 K upon 280 nm excitation in which the ranges of integration were marked. For all the spectra, integrated intensities of three emissions of Pr^{3+}: 5d→4f (I_{df}), $^3P_0 \rightarrow {}^3H_4$ (I_{3P0}), and $^1D_2 \rightarrow {}^3H_4$ (I_{1D2}), were calculated, see **Figure 4b**.

Consequently, three thermometric parameters (Δ_1-Δ_3) were defined according to **Eq. (6)**

$$\Delta_1 = \frac{I_{df}}{I_{1D2}}, \qquad \Delta_2 = \frac{I_{df}}{I_{3P0}}, \qquad \Delta_3 = \frac{I_{3P0}}{I_{1D2}}. \qquad \textbf{(6)}$$

Temperature dependence of the $\Delta_1 - \Delta_3$ parameters is shown in **Figure 5**. The experimental data represented by Δ_1 and Δ_2 were fitted using Mott-Seitz model described by **Eq. (7)** [25,26]

$$\Delta_{1,2} \approx \frac{\Delta_0}{1 + \sum_{i=1}^{N} \alpha_i \exp\left(\frac{-E_{ai}}{k_B T}\right)}. \qquad \textbf{(7)}$$

In **Eq. (7)**, Δ_0 is the Δ parameter at the limit $T \rightarrow 0$ K, $\alpha_i = W_{0i}/W_{Ri}$ is the ratio of the nonradiative (W_{0i} at $T \rightarrow 0$ K) and radiative (W_{Ri}) rates and E_{ai}, is the energy barrier value for the non-radiative relaxations. The Mott-Seitz model with $N = 3$ was chosen due to the double S-shape of the experimental points and various rates of thermal quenching of the Pr^{3+} luminescence [11].

Obviously, the values of the parameters derived from the fits, such as activation energies, have little physical meaning as the experimental data come from a mixture of two phosphors. In each of them, the radiative and non-radiative processes depend differently on temperature. The same applies to thermal quenching of the 5d→4f luminescence and thus, the temperature dependence of its decay time [27]. Nevertheless, **Eq. (7)** allowed obtaining a perfect fit of the experimental data for both thermometric parameters, with r^2=0.999, see **Figure 5 and Table 1**. The accomplished fits may then serve as perfect calibration curves for thermometric purposes.

Finding the calibration curve for Δ_3 (**Eq. (3)**) could not be attained using the Mott-Seitz model. To find the most accurate physical approach in this case it is necessary to solve the rate equations as reported by Suta [22] and Geitenbeek [28]. Yet, for the purpose of this work and taking into account that the thermometer under investigation is a mixture of two phosphors we considered it unfounded and redundant.

Consequently, to fit the Δ_3 thermometric parameter (**Eq. (6)**), an exponential function with A_1, t_1, and t_2 fitting parameters, described by **Eq. (8)** was used.

$$\Delta_3 = A_1 exp\left(\frac{-T_1}{t_1}\right) + A_2 exp\left(\frac{-T_2}{t_2}\right) + A_0. \qquad \textbf{(8)}$$

This function allows obtaining an excellent fit of the experimental data, with r^2 not lower than 0.999, see **Figure 5 and Table 1**.

The temperature dependence of S_r and δT for $\Delta_1 - \Delta_3$ is presented in **Figure 6**. The highest value of the S_r (S_m) was obtained for Δ_1 and reached 1.65 %·K^{-1} at 40 K. S_m = 0.80 %·K^{-1} at 52 K (for Δ_2) and S_m = 0.80

%·K^{-1} at 15 K (for Δ_3) were obtained. The thermometric parameters are slightly lower than in the case of the two individual phosphors investigated previously [11], but it was expected, as mentioned in the Introduction. More importantly, the YAGG-mix system offers the possibility of temperature sensing, independently of which of the thermometric parameter (delta1 -delta3) is used, in the broad range of temperatures, 15-675 K.

Using temperature dependence of the 5d→4f luminescence decay time, see **Figure 3**, S_r and δT were also calculated according to the **Eqs. (3)** and **(4)** and the results are presented in **Figure 7**. When the 5d→4f luminescence decay time is a thermometric parameter, S_r grows from 0.007 %·K^{-1} at 250 K to 0.6 %·K^{-1} at 630 K, and the operating range covers the 250-650 K. The values of δT are low and do not exceed 0.014 K at the S_m (at temperature as high as 630 K). One might reasonably expect that higher content of the $Y_3(Al_1Ga_4)O_{12}$:0.1%Pr in the mixture might extent the low-temperature limit of the operating range towards lower temperatures. Hence, the decay time of the 5d→4f luminescence of the YAGG-mix may be considered the fourth thermometric parameter of this luminescence thermometer.

Table 2 summarizes the present findings and compares them with the thermometric performance of the two individual Ga-modified garnets: ($Y_3(Al_3Ga_2)O_{12}$:0.1%Pr and $Y_3(Al_1Ga_4)O_{12}$:0.1%Pr) [11]. For single-composition Ga-modified garnets, S_m are higher than for the YAGG-mix when Δ_1 is considered as a thermometric parameter. Namely, for the $Y_3(Al_3Ga_2)O_{12}$:0.1%Pr S_m = 2.3 %·K^{-1} at 345 K and for the $Y_3(Al_1Ga_4)O_{12}$:0.1%Pr S_m = 3.6 %·K^{-1} at 60 K. Taking into account Δ_3 thermometric parameter for the YAGG-mix, S_m = 0.80 %·K^{-1} at 15 K, while for the $Y_3(Al_3Ga_2)O_{12}$:0.1%Pr and $Y_3(Al_1Ga_4)O_{12}$:0.1%Pr S_m is lower; 0.6 %·K^{-1} at 700 K and 0.3 %·K^{-1} at 520 K, respectively. Yet, the YAGG-mix presents indeed a flatter temperature-dependence of S_r than the individual phosphors and shows the regularly higher minimal value of S_r, which is an obvious advantage of this thermometer.

For all the LIR-related thermometric parameters ($\Delta_1 - \Delta_3$) the operating range of the YAGG-mix spans the 15-675 K range with still good maximal relative sensitivity showing reasonably flat course over the

whole measuring range, as just discussed. The δT is also very satisfying for the YAGG-mix allowing to measure with good accuracy over such a broad range of temperatures, see **Table 2** and **Figure 6**. The individual phosphors, $Y_3(Al_3Ga_2)O_{12}$:0.1%Pr and $Y_3(Al_1Ga_4)O_{12}$:0.1%Pr, presented even four times higher maximal temperature uncertainties in the case of Δ_3, while for Δ_1 and Δ_2 the values for single phosphor and for the YAGG-mix the values were quite similar (see **Table 2**). This is an unexpectedly significant gain of the quality of temperature measurement executing the YAGG-mix.

Conclusions

This paper presents the temperature-dependent photoluminescence of the mixture of $Y_3(Al_3Ga_2)O_{12}$:0.1%Pr and $Y_3(Al_1Ga_4)O_{12}$:0.1%Pr Ga-modified garnets and its performance in luminescence thermometry. The YAGG-mix showed strong photoluminescence (5d→4f, $^3P_0 \rightarrow {}^3H_{4,5}$, and $^1D_2 \rightarrow {}^3H_{4,5}$) whose temperature dependence was utilized in temperature sensing. The presented results proved that by mixing phosphors possessing the same crystallographic structure and activated with the same luminescence ion (Pr^{3+}), it is possible to formulate a high-quality luminescence thermometer. By deliberately selecting phosphors for the mixture, it is possible to significantly modify and control such luminescent properties as the relative intensities of particular emission bands and their thermal quenching. Using the intensity ratio of 5d→4f and $^1D_2 \rightarrow {}^3H_4$ luminescence of Pr^{3+} the highest S_m=1.65 %·K^{-1} at 40 K was obtained. Independently on the thermometric parameter ($\Delta_1 - \Delta_3$), the operating range of the mixed garnets covered a 15-675 K range which was limited by our setup and not by the thermal intrinsic characteristics of the phosphors. In the case of the single $Y_3(Al_3Ga_2)O_{12}$:0.1%Pr and $Y_3(Al_1Ga_4)O_{12}$:0.1%Pr garnets such flexibility is not offered. In the whole operating range, the temperature uncertainties of the YAGG-mix were either four times better or at similar level as for the individual $Y_3(Al,Ga)_5O_{12}$:0.1%Pr garnets depending on the thermometric parameters under consideration. From this research, the most promising and prospective advantage of the mixed phosphors is the possibility of widening of the operating range of the luminescence thermometers combined with low measurement resolution when the three LIR thermometric parameters are used. Especially high gain of the quality of temperature measuring with YAGG-mix was achieved exploiting the

5d→4f luminescence decay time for which the resolution of the temperature sensing never exceeded 0.11 K. The idea of mixing phosphors of the same crystal structure and activated with the same dopant can be considered as a new concept in designing novel luminescent thermometers of well-controlled performance.

Acknowledgments:

This research was supported by the Polish National Science Centre (NCN) under grants #UMO-2017/25/B/ST5/00824 and 2018/29/B/ST5/00420. This work was also developed within the scope of the project CICECO – Aveiro Institute of Materials, UIDB/50011/2020, financed by Portuguese funds through the FCT/MEC and when appropriate co-financed by FEDER under the PT2020 Partnership Agreement. The financial support from the project NanoHeatControl, POCI-01-0145-FEDER-031469, funded by FEDER, through POCI and by Portuguese funds (OE), through FCT/MCTES, and by European Union's Horizon 2020 FET Open program under grant agreements no. 801305 are acknowledged. E. Z. and L. D. C. are grateful to the Polish National Agency for Academic Exchange (NAWA) for support under the NAWA-Bekker #PPN/BEK/2018/1/00333/DEC/1 and NAWA-Ulam #PPN/ ULM/2019/1/00077/U/00001 projects, respectively.

Figures

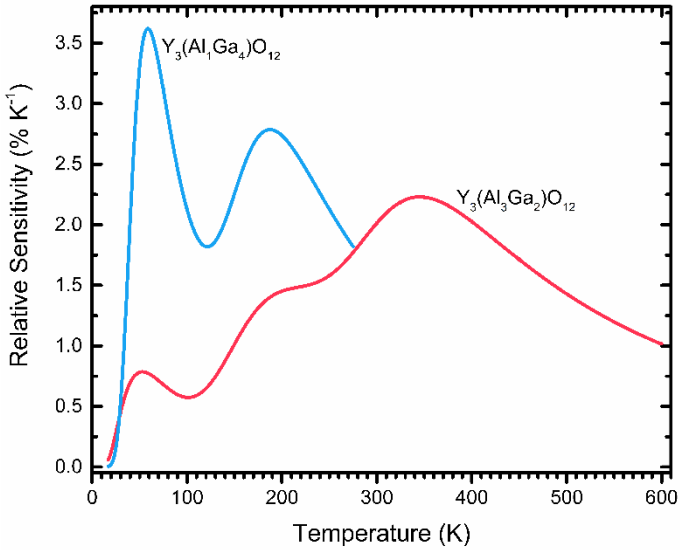

Figure 1. Relative sensitivities of Ga-modified garnets; $Y_3(Al_3,Ga_2)O_{12}$:0.1%Pr and $Y_3(Al_1,Ga_4)O_{12}$:0.1%Pr for $\boldsymbol{\Delta_1}$ thermometric parameter.

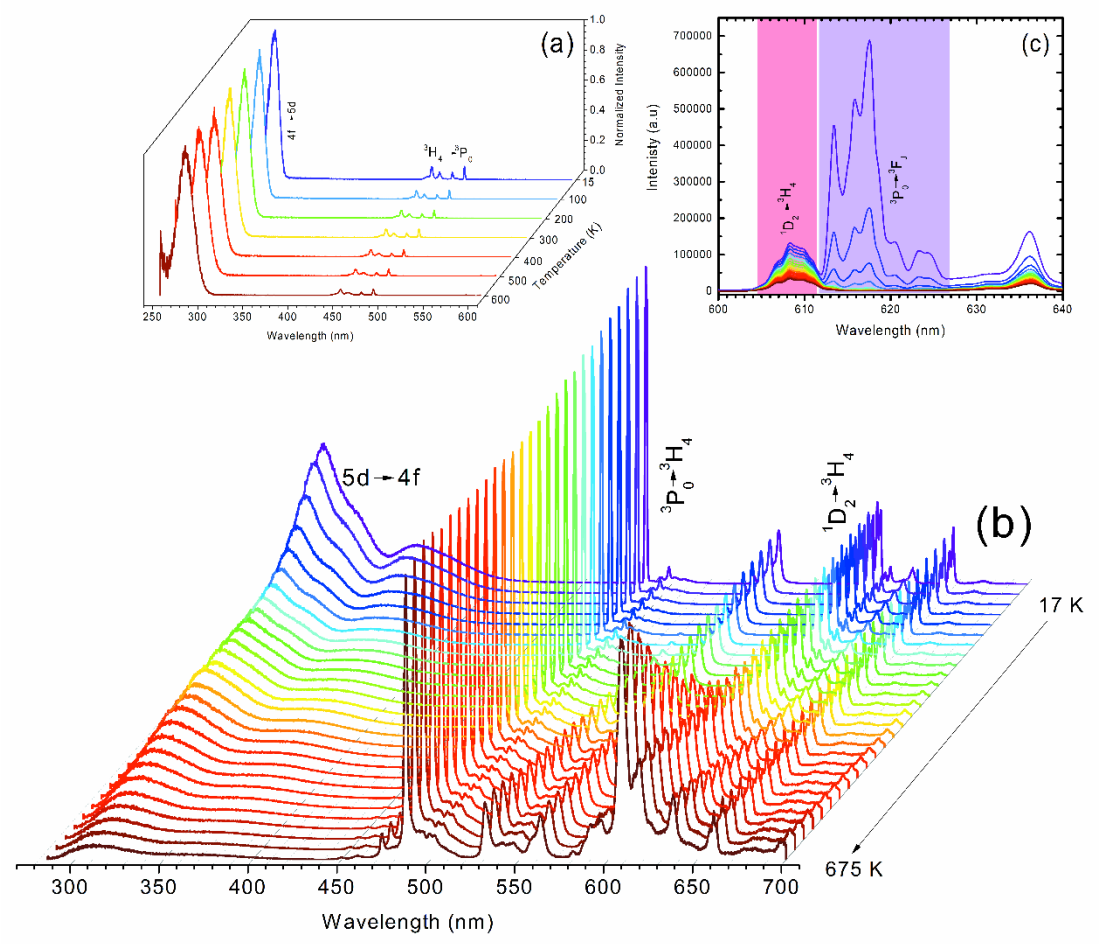

Figure 2. (a) Excitation spectra of 606.3 nm luminescence of Pr^{3+} registered at various temperatures for the YAGG-mix. (b) Emission spectra registered under 280 nm at various temperatures (15-675 K). All the spectra were normalized at 486 nm ($^3P_0$ luminescence). (c) Time Resolved Emission Spectroscopy (TRES) registered under 280 nm excitation at 15 K for the YAGG-mix.

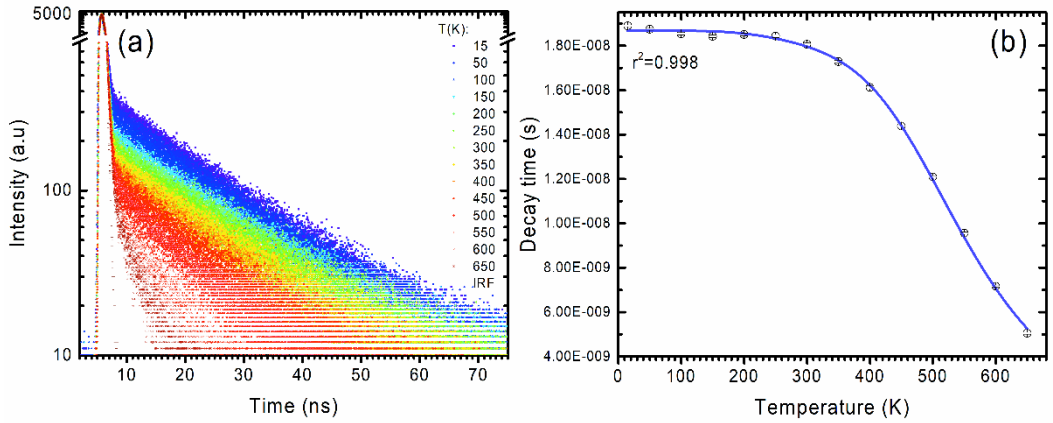

Figure 3. (a) Decay traces of 5d→4f luminescence of Pr^{3+}. Decay traces were taken under 280 nm excitation in the 15-650 K range of temperature. (b) Temperature dependence of 5d→4f decay times of Pr^{3+} registered for the YAGG-mix.

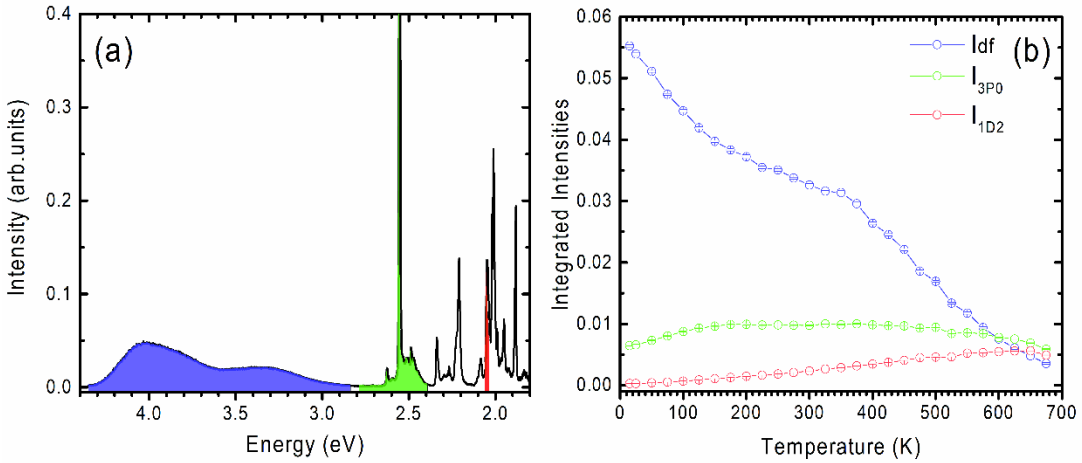

Figure 4. (a) Luminescence spectrum of the YAGG-mix registered at 300 K. Areas of integration of the three emissions of Pr^{3+} (5d→4f, $^3P_0 \rightarrow {}^3H_4$, and $^1D_2 \rightarrow {}^3H_4$) are indicated with violet, green and red color, respectively. (b) Temperature dependence of the integrated intensities of the three luminescence bands of Pr^{3+} in the YAGG-mix.

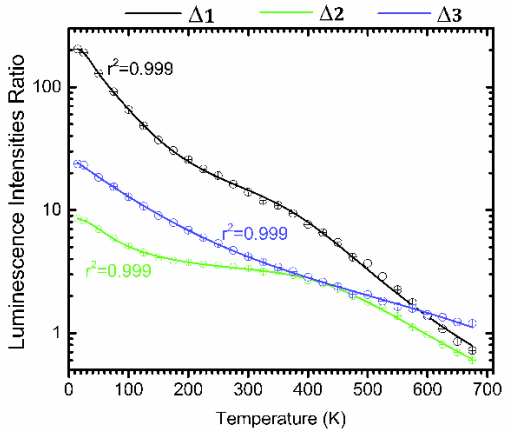

Figure 5. Calibration curves of the YAGG-mix using $\boldsymbol{\Delta_{1-3}}$. Solid lines represent the fits to the experimental data using the Mott-Seitz model for $\boldsymbol{\Delta_1}$ and $\boldsymbol{\Delta_2}$ and exponential function for $\boldsymbol{\Delta_3}$.

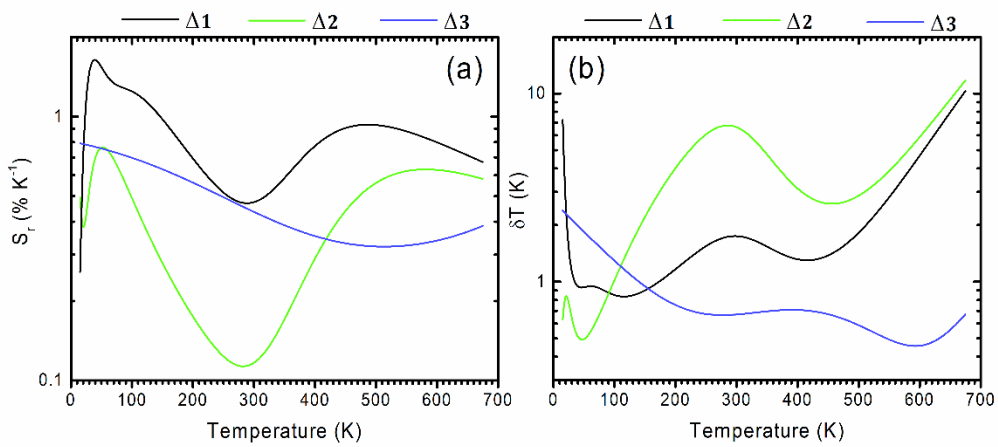

Figure 6. Temperature dependence of the **(a)** relative sensitivity and **(b)** temperature uncertainty for the YAGG-mix using $\Delta_{1\text{-}3}$ thermometric parameters.

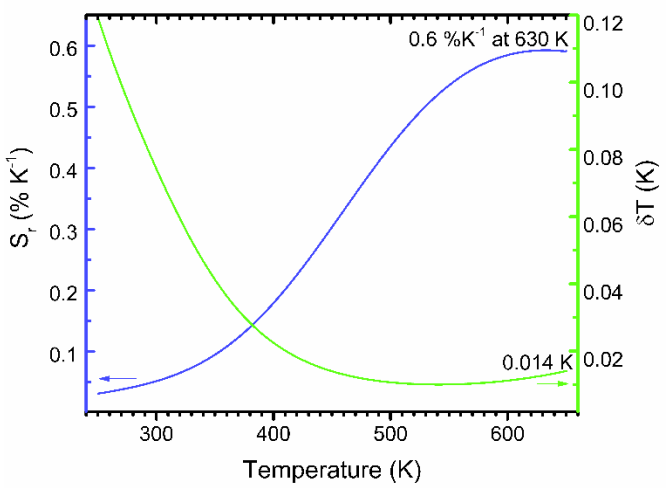

Figure 7. Relative sensitivity and temperature uncertainty for the YAGG-mix using decay time of the 5d→4f luminescence of Pr^{3+} as a thermometric parameter.

Table 1. Fitting parameters of $\boldsymbol{\Delta_1 - \Delta_3}$ experimental data

y=(A/(1+(B*(exp(-(C/(k*x)))))+(D*(exp(-(E/(k*x)))))+(F*(exp(-(G/(k*x)))))))		
$\boldsymbol{\Delta_1}$		
Parameter	**R^2**	**Value**
A	0.9999	204±1
B		41±2
C		0.04±0.001
D		4.3±0.2
E		0.0090±2E-4
F		34084±18068
G		0.29±0.02
k		8.61733E-5±0
$\boldsymbol{\Delta_2}$		
Parameter	**R^2**	**Value**
A	0.999	9.2±0.2
B		1701±321
C		0.29±0.01
D		0.18±0.03
E		0.0011±5E-4
F		2.5±0.1
G		0.0114±4E-4
k		8.61733E-5±0
y = A1*exp(-x/t1) + A2*exp(-x/t2) + A0		
$\boldsymbol{\Delta_3}$		
Parameter	**R^2**	**Value**
A0	0.999	0±0
A1		20±1
t1		99±7
A2		7±1
t2		370±53

Table 2. Comparison of thermometric parameters for $Y_3(Al_3Ga_2)O_{12}$:0.1%Pr, $Y_3(Al_1Ga_4)O_{12}$:0.1%Pr, and the YAGG-mix phosphors.

Thermometric parameter	*Performance of luminescence thermometers*			
	range of S_r (%•K^{-1})	T_m (K)	range of δT (K)	ΔT (K)
YAGG-mix				
$\boldsymbol{\Delta_1}$	0.25-1.65	40	0.8-10	15-675
$\boldsymbol{\Delta_2}$	0.1-0.8	52	0.5-12	15-675
$\boldsymbol{\Delta_3}$	0.4-0.8	15	0.4-2.4	15-675
$\boldsymbol{\tau}$	0.03-0.6	630	0.014-0.1	250-650
$Y_3(Al_3Ga_2)O_{12}$:0.1%Pr				
$\boldsymbol{\Delta_1}$	0-2.3	345	0.03-4	17-600
$\boldsymbol{\Delta_2}$	0-1.7	220	0.03-10	50-600
$\boldsymbol{\Delta_3}$	0.15-0.6	700	0.2-10	290-700
$\boldsymbol{\tau}$	0.1-1.2	480	0.002-0.05	300-600
$Y_3(Al_1Ga_4)O_{12}$:0.1%Pr				
$\boldsymbol{\Delta_1}$	0-3.6	60	0.03-3	17-275
$\boldsymbol{\Delta_2}$	0.1-2.0	145	0.05-10	19-275
$\boldsymbol{\Delta_3}$	0.01-0.3	520	0.02-6	17-580
$\boldsymbol{\tau}$	0.1-1.4	184	0.02-0.1	15-275

References

[1] P. Dorenbos, Energy of the first 4f7-4f65d transition of Eu2+ in inorganic compounds, 104 (2003) 239–260. doi:10.1016/S0022-2313(03)00078-4.

[2] C.D.S. Brites, A. Millán, L.D. Carlos, Lanthanides in Luminescent Thermometry, Handbook on the Physics and Chemistry Of Rare Earths, 49 (2016) 339–427.

[3] D. Jaque, F. Vetrone, Luminescence nanothermometry, Nanoscale. 4 (2012) 4301. doi:10.1039/c2nr30764b.

[4] M.D. Dramićanin, Luminescence Thermometry Methods, Materials, and Applications, Woodhead Publishing, 2018.

[5] C.D.S. Brites, S. Balabhadra, L.D. Carlos, Lanthanide-Based Thermometers: At the Cutting-Edge of Luminescence Thermometry, Adv. Opt. Mater. 7 (2019) 1801239. doi:10.1002/adom.201801239.

[6] M.D. Dramićanin, Trends in luminescence thermometry, J. Appl. Phys. 128 (2020) 040902. doi:10.1063/5.0014825.

[7] M. Grinberg, The radiative processes in chromium-doped systems with strong electron—phonon coupling, Phys. Status Solidi. 130 (1992) K189–K193. doi:10.1002/pssa.2211300243.

[8] A. Bednarkiewicz, L. Marciniak, L.D. Carlos, D. Jaque, Standardizing luminescence nanothermometry for biomedical applications, Nanoscale. 12 (2020) 14405–14421. doi:10.1039/D0NR03568H.

[9] M.D. Dramićanin, Sensing temperature via downshifting emissions of lanthanide-doped metal oxides and salts. A review, Methods Appl. Fluoresc. 4 (2016) 042001. doi:10.1088/2050-6120/4/4/042001.

[10] Y. Zhao, X. Wang, Y. Zhang, Y. Li, X. Yao, Optical temperature sensing of up-conversion luminescent materials: Fundamentals and progress, J. Alloys Compd. 817 (2020) 152691. doi:10.1016/j.jallcom.2019.152691.

[11] P. Bolek, J. Zeler, C.D.S. Brites, J. Trojan-piegza, L.D. Carlos, E. Zych, Ga-modified YAG : Pr 3 + dual-mode tunable luminescence thermometers, Chem. Eng. J. 421 (2021) 129764. doi:10.1016/j.cej.2021.129764.

[12] S. Wang, S. Ma, G. Zhang, Z. Ye, X. Cheng, High-Performance Pr3+ -Doped Scandate Optical Thermometry: 200 K of Sensing Range with Relative Temperature Sensitivity above 2%·K –1, ACS Appl. Mater. Interfaces. 11 (2019) 42330–42338. doi:10.1021/acsami.9b13873.

[13] C.D.S. Brites, K. Fiaczyk, J.F.C.B. Ramalho, M. Sójka, L.D. Carlos, E. Zych, Widening the Temperature Range of Luminescent Thermometers through the Intra- and Interconfigurational Transitions of Pr 3+, Adv. Opt. Mater. 6 (2018) 1701318. doi:10.1002/adom.201701318.

[14] M. Sójka, J.F.C.B. Ramalho, C.D.S. Brites, K. Fiaczyk, L.D. Carlos, E. Zych, Bandgap Engineering and Excitation Energy Alteration to Manage Luminescence Thermometer Performance. The Case of Sr 2 (Ge,Si)O 4 :Pr 3+, Adv. Opt. Mater. 7 (2019) 1901102. doi:10.1002/adom.201901102.

[15] M. Sójka, C.D.S. Brites, L.D. Carlos, E. Zych, Exploiting bandgap engineering to finely control dual-mode Lu2 (Ge,Si)O5:Pr3+ luminescence thermometers, J. Mater. Chem. C. 8 (2020) 10086–10097. doi:10.1039/D0TC01958E.

[16] M. Sekulić, V. Đorđević, Z. Ristić, M. Medić, M.D. Dramićanin, Highly Sensitive Dual Self-

Referencing Temperature Readout from the Mn4+/Ho3+ Binary Luminescence Thermometry Probe, Adv. Opt. Mater. 6 (2018) 1800552. doi:10.1002/adom.201800552.

[17] D. Avram, C. Colbea, M. Florea, C. Tiseanu, Highly -sensitive near infrared luminescent nanothermometers based on binary mixture, J. Alloys Compd. 785 (2019) 250–259. doi:10.1016/j.jallcom.2019.01.162.

[18] L. Zhao, B. Lou, J. Mao, B. Jiang, X. Wei, Y. Chen, M. Yin, Optical temperature sensing properties of a phosphor mixture of Sr2Mg3P4O15:Eu2+ and SrB4O7:Sm2+, Mater. Res. Bull. 109 (2019) 103–107. doi:10.1016/j.materresbull.2018.09.032.

[19] C. Xie, P. Wang, Y. Lin, X. Wei, M. Yin, Y. Chen, Temperature-dependent luminescence of a phosphor mixture of Li2TiO3: Mn4+ and Y2O3: Dy3+ for dual-mode optical thermometry, J. Alloys Compd. 821 (2020) 153467. doi:10.1016/j.jallcom.2019.153467.

[20] G. Blasse, B.C. Grabmaier, Luminescent Materials, Springer-Verlag, Berlin Heidelberg, 1994.

[21] J. Mooney, P. Kambhampati, Get the Basics Right: Jacobian Conversion of Wavelength and Energy Scales for Quantitative Analysis of Emission Spectra, J. Phys. Chem. Lett. 4 (2013) 3316–3318. doi:10.1021/jz401508t.

[22] M. Suta, A. Meijerink, A Theoretical Framework for Ratiometric Single Ion Luminescent Thermometers—Thermodynamic and Kinetic Guidelines for Optimized Performance, Adv. Theory Simulations. 3 (2020) 2000176. doi:10.1002/adts.202000176.

[23] C.D.S. Brites, P.P. Lima, N.J.O. Silva, A. Millan, F. Palacio, V.S. Amaral, L.D. Carlos, Nanoscale Thermometry at the nanoscale, Nanoscale. 4 (2012) 4799–4829. doi:10.1039/c2nr30663h.

[24] M. Jia, Z. Sun, M. Zhang, H. Xu, Z. Fu, What determines the performance of lanthanide-based ratiometric nanothermometers?, Nanoscale. 12 (2020) 20776–20785.

[25] N.F. Mott, On the absorption of light by crystals, Proc. R. Soc. LONDON Ser. A. 167 (1938) 384.

[26] D. Ananias, F.A.A. Paz, D.S. Yufit, L.D. Carlos, J. Rocha, Photoluminescent Thermometer Based on a Phase-Transition Lanthanide Silicate with Unusual Structural Disorder, J. Am. Chem. Soc. 137 (2015) 3051–3058. doi:10.1021/ja512745y.

[27] J. Ueda, A. Meijerink, P. Dorenbos, A.J.J. Bos, S. Tanabe, Thermal ionization and thermally activated crossover quenching processes for 5d-4f luminescence in Y3Al5-xGaxO12:Pr3+, Phys. Rev. B. 95 (2017) 014303. doi:10.1103/PhysRevB.95.014303.

[28] R.G. Geitenbeek, H.W. de Wijn, A. Meijerink, Non-Boltzmann Luminescence in NaYF4:Eu3+: Implications for Luminescence Thermometry, Phys. Rev. Appl. 10 (2018) 064006. doi:10.1103/PhysRevApplied.10.064006.